Int J Med Rev 2024 December;11(4): 830-841

10.30491/IJMR.2025.497228.1299

INTERNATIONAL JOURNAL OF MEDICAL REVIEWS

Original Article

Green Synthesis of Silver Nanoparticles from *Glycine max* Pods: Potential Anti-Cancer Activity Against Hepatocellular Carcinoma

Syeda Saba Batool [1], Aneela Anwar [1*], Amna Shoaib [2], Shamsa Mubeen [3], Azeem Intisar [4], Shahzeb Khan [5], Mohsin Kazi [6]

[1] Department of Chemistry, University of Engineering and Technology, Lahore,54890, Pakistan
[2] Department of Plant Pathology, University of the Punjab, Lahore, 54000, Pakistan
[3] Department of Biochemistry & Molecular Biology, University of Gujrat,50700, Pakistan
[4] School of Chemistry, University of Punjab, Quiad-e-Azam Campus, Lahore, 54000, Punjab, Pakistan
[5] Center of Pharmaceutical Engineering Science, Faculty of Life Science, School of Pharmacy, University of Bradford, BD7 1DP, UK
[6] Department of Pharmaceutics, College of Pharmacy, King Saud University, P.O. BOX 2457; Riyadh 11451, Saudi Arabia

*** Corresponding Author:** Aneela Anwar, Department of Chemistry, University of Engineering and Technology, Lahore,54890, Pakistan. E-mail: a.anwar@uet.edu.pk

Received November 1, 2024; **Accepted** December 27, 2024; **Online Published** December 30, 2024

Abstract

Introduction: Hepatocellular carcinoma, represents one of the greatest burdens in the oncology domain, with a significant negative global health and mortality rates. *Glycine max*, a plant used for centuries in various traditional medicine approaches, has shown good anti-cancer potential. The main objective of study was to analyse the anti-cancer activity of nanoparticle of *Glycine max*.

Methods: Nanoparticles were synthesized with *Glycine max* pods extract and a silver nitrate aqueous solution. Moreover, these are characterized via SEM-EDX, UV, XRD, and DLS analysis. Cell viability and cytotoxicity of bioinspired AgNPs was accessed using MTT as well as the trypan blue assay.

Results: Structural alterations of HepG2 cells were analysed by phase contrast microscope, showing significant results at a dose of 30 µg/ml. The upregulated expression of Annexin-V protein confirms that cell death occurred through apoptosis.

Conclusion: *Glycine max* has demonstrated its capability to produce AgNPs with apoptotic activities *in vitro*, offering a promising and economical solution for potentially combating hepatocellular carcinoma.

Keywords: Hepatocellular carcinoma, *Glycine max*, Nanoparticles, Apoptosis, Bioinspired

Introduction

Nanoscience studies the creation, composition, and control of small materials, ranging from 1 to 100 nanometers.[1] Nanotechnology is rapidly expanding, with applications in biotechnology,[2] textiles,[3] cosmetics, and medicine. Nanoparticles show promise in biosensors, drug transport, diagnostic tools, and cancer therapy.[4]

Hepatocellular carcinoma, more commonly known as HCC, remains an important contributing factor to cancer-related fatalities on around the world, with a significant portion of cases being diagnosed at advanced stages, resulting in poor treatment outcomes.[5,6] Only 30-40% of HCC patients are eligible for potentially therapeutic treatments such as liver transplantation, tumor dissection, or radiofrequency ablation at the time of diagnosis.

The majority of individuals often must endure non therapeutic interventions such as transcatheter arterial chemoembolization (TACE).[6] Bioinspired nanoparticles have been engineered to mimic the properties of biological systems, such as cell membranes, to enhance their tumor-homing ability and biocompatibility. These nanoparticles have demonstrated synergistic anticancer effects through simultaneous chemotherapy, hyperthermia -therapy, and radiotherapy can be administered without any harmful side effects.[7]

Glycine max, commonly known as soybeans, are a rich source of bioactive compounds with potential therapeutic applications. The pods of soybeans contain a variety of bioactive molecules, including flavonoids, phenolic acids, and saponins, which have been linked to antioxidant, anti-inflammatory, and antimicrobial

properties.[8,9]

Silver nanoparticles (AgNPs) have demonstrated significant potential as both antimicrobial and anticancer agents, making them a promising candidate for cancer therapy. The bioinspired approach employed in this study, which utilizes the bioactive compounds present in *Glycine max* (soybean) pods to facilitate the synthesis of AgNPs, provides numerous benefits over conventional chemical-based techniques for synthesis i.e., reduced environmental impact, Enhanced therapeutic potential and improved efficacy.[10-12]

Hepatocellular carcinoma is a challenging condition characterized by severe inflammation and significant pain, complicating the disease for patients. Among the primary risk aspects for HCC, the most usual histological type of primary liver cancer is infection with the hepatitis B virus or the hepatitis C virus (Rumgay *et al.*, 2022).

In addition to hepatitis B and hepatitis C virus infections, hepatocellular carcinoma (HCC) can also be triggered by other factors such as excessive alcohol consumption, obesity, diabetes, and exposure to aflatoxins.

Hepatitis B and C collectively affect hundreds of millions of people worldwide, primarily leading to chronic diseases. They stand as the primary causes of liver cirrhosis, liver cancer, and fatalities associated with viral hepatitis. Hepatitis B and C infect around 354 million individuals worldwide, yet accounting for the majority of these patients receives screened and treated (WHO).

Hepatitis B virus infection is responsible for about 60% of all liver cancers worldwide in developing countries, while hepatitis C virus infection is responsible for 33% of all liver cancer cases (Liu *et al.*, 2015).

There are several treatment choices for patients with hepatocellular carcinoma. The best plan would be based on the stage of cancer at diagnosis, the underlying liver function of the patient, and the patient's overall health. This treatment often entails several specialists collaborating to provide the best comprehensive care for an HCC patient. The team may include a surgeon, oncologist, hepatologist, interventional radiologist, and palliative care provider. This multi-disciplinary strategy aims to offer the outstanding score care based on each particular patient (Mokdad *et al.*, 2016).

This study offers a novel approach to the treatment of liver cancer by using *Glycine max* nanoparticles over HepG2 cell line (*in-vivo* treatment) that may improve patient care by extending life expectancy, controlling symptoms, and improving quality of life in general.

Materials and Methods

Materials

The materials were utilized for this study encompass *Glycine max* pods, which served as a primary source for the bioactive compounds. Double distilled water was utilized for all aqueous preparations to ensure purity. Silver nitrate (Sigma-Aldrich, ≥99.5%) was employed as a precursor for nanoparticle synthesis. A 70% ethanol solution was used for sterilization purposes.

For cell culture, DMEM media (13.37 g/L, Sigma, USA, or Capricorn Scientific) was supplemented with 0.0037 g/L sodium bicarbonate, 200-300 units/L of Penicillin/Streptomycin (Sigma, USA), and 200 units/L of Gentamicin to maintain sterility. Fetal Bovine Serum (FBS) at 10% concentration (27 ml) from Sigma, USA, was also incorporated into the cell culture media. HepG2 cancer cell lines were used to assess cytotoxicity and other biological activities.

Trypan blue (Invitrogen Inc., USA) was employed for cell viability assays, and a 0.1% crystal violet dye blended with 2% ethanol was used for cell staining.

To solubilize the stain, 1% SDS was used. Experiments were conducted in 96-well plates (Corning, USA). VEGF and Annexin V kits (Santa Cruz Biotechnology, USA) were used for ELISA assays. A 0.18 M sulfuric acid (H_2SO_4) solution was prepared for the TMB assay (Invitrogen Inc., USA), and an LDH assay kit (AMP Diagnostics, Austria) was used to measure cell injury. For cell subculturing, 0.05% trypsin and 0.53 mM EDTA were utilized. Additional solutions included PBS (Invitrogen Inc., USA) for washing, MTT solution (Invitrogen Inc., USA) for cell proliferation assays, and DMSO (Invitrogen Inc., USA) for dissolving formazan crystals in the MTT assay.

Methodology

Botanical Specimen Collection & Preparation of Extract

Glycine max samples obtained from the Lahore local market were washed with water and cleaned followed by drying at 40 °C in muffle furnace and powdered in grinder, after that, 20 g of each dried material was extracted in 100 ml double-distilled water and boiled at

100 °C for 10 min. Later, filtered extracts were centrifuged for 15 at the speed of 4000 rpm and stored at 4 °C, Soxhlet apparatus was used for it.

Synthesis of Bioinspired Glycine max AgNPs

A flask containing 20 ml of 5mM silver nitrate was combined with 70 ml of a 20 percent *Glycine max* pods solution, and continuous stirring was conducted at 24 °C for 4 h. A color shift signalizing the formation of *Glycine max*-Derived Nanoparticle resulted from this process. The product solution centered after spinning at 4000 rpm for 20 minutes, and the pellet was cleansed twice, dried at 50 °C, and the *Glycine max*-Derived Nanoparticles were calcined for 2 h at 500 °C in a muffle furnace.

Analytical Characterization of Bioinspired AgNPs

The Ultraviolet-visible spectrophotometer UV-Vis was employed in the characterization of *Glycine max*-Derived Nanoparticles. The UV-visible spectra collection was in 250-750 nm wavelength.

The dynamic light scattering DLS technique to determine the zeta potential and particle size distribution of the synthesized sample were calculated using Litesizer DLS 500 instrument. FTIR spectrophotometer on wave number regions from 4000-600 cm^{-1} was utilized in conducting the functional group analysis of *Glycine max*-Derived Nanoparticles.

Scanning Electron Microscopy-Energy Dispersive X-RAY SEM-EDX study conducted to investigate the surface morphology structural and elemental composition of the green synthesized *Glycine max*-Derived Nanoparticles.

The crystalline average size of *Glycine max*-Derived Nanoparticles was determined using X-ray diffraction XRD analysed.

Laboratory Setting Anticancer Efficacy Regarding Bioinspired AgNPs

Managing the Cell Line through Sub-Culturing

The HepG2 cells from CAMB, Lahore, were cultured in DMEM-HG and underwent subculturing when they reached 70-80% confluence. This required the use of trypsin-EDTA treatment, verifying detachment through microscopic observation, and centrifuging at 12000 rpm about 10 minutes. The extracellular fluid proved carefully extracted, displacing the cell pellet that was mixed with 10% serum and DMEM.

Treatment of HepG2 Cell Line with Bioinspired AgNPs

HepG2 cells that had been pre-conditioned with nanoparticles derived from *Glycine max* were divided into two groups. The initial group was comprised of normal cells grown in standard medium, while the second group consisted of treated cells grown in the *Glycine max*-derived nanoparticles. During a span of 72 h, samples were gathered for ELISA, cell proliferation, lactate dehydrogenase assay (LDH), and viability assays.

Enzyme-Linked Immunosorbent Assay (ELISA)

A solid-phase sandwich ELISA was conducted in a 96-well plate to detect the presence of VEGF and Annexin V markers. After incubating with antibodies and performing necessary steps such as washing and blocking, the culturing medium was added and then removed after 30 min. Throughout a 60-min incubation period, the sample underwent treatment with an HRP-conjugated donkey anti-rabbit secondary antibody. This was followed by three thorough washes and the subsequent detection process involved the use of Tetramethylbenzidine (TMB). The reactivity was halted by incorporating 100 µl of 0.18 M sulphuric acid, and its absorbance was then evaluated at 450 nm via the microtiter plate.

LDH Assay

The LDH activity in the medium obtained from all study groups, as well as 5 µl of medium from each cell line group following treatment completion, was assessed using an LDH assay reagent. The assay was conducted following the instructions provided by the manufacturer.

For a brief incubation period of 5 min, a tiny amount of medium for cultivating cells to every group was utilized with a larger volume of working reagent. The reaction was then halted by adding 90 µl of 1N HCl. After that, the mixture was divided into cuvettes while absorbance has been measured via a spectrophotometer that was calibrated at 490 nm.

Cell Proliferation Assay

An MTT assay was performed to evaluate the expansion capabilities of the HepG2 cell line groups. The cell monolayer was treated with PBS, then incubated in 500 µl of complete medium with 60 µl of

MTT solution for 2 h. The resulting purple formazan was dissolved using dimethylsulfoxide (DMSO), and the absorbance was measured at 570 nm.

Cell Viability Assay

The viability of the cells was evaluated via the use of trypan blue dye after rinsing them with PBS. After a 15-min incubation and three more PBS washes, the cells were scrutinized under a microscope. Cells dyed via trypan blue were determined to be non-viable, and the percentage of viable cells was calculated using a hemocytometer.

Crystal Violet Staining

The assessment of cell viability was conducted through the utilization of crystal violet staining across a 6-well plate. A medium was added concerning altered groups for trails of HepG2 cell line-derived cells into separate wells. After incubation, the medium in each well of the plate was discarded and then rinsed with PBS. After that, wells were treated with a solution containing 2% ethanol and 0.1% crystal violet dye, making sure to cover the entire surface. Completely filled.

The plate was then left to incubate for 15 min at room temperature. Afterwards, the excess dye was carefully eliminated, while channels were gently cleansed to ensure the cells on the surface remained intact. Next, in order to dissolve the stain, 600 µl of 1% SDS was added to each well, and then left to incubate for 5-10 min. The absorbance was measured using a microtiter plate reader at 540 nm.

Data Analysis Using Statistical Approaches

The statistical evaluation utilized one-way ANOVA, with Bonferroni's test for group associations. Analysis was conducted by means of GraphPad v9.5 software, alongside the standard of significance set at $P<0.05$.

Results

Green synthesis of nanoparticles is gaining attention in the biomedical applications of nanoparticles for their eco-sensitive and possible biocompatible nature. The current green-synthesized nanoparticles; *Glycine max*-derived nanoparticles were used for the anti-proliferative and apoptotic activity in hepatocellular carcinoma. Various characterization techniques used in the current study can offer better understanding and explanation of how the synthesized nanoparticles might be working in cancer cells through their physicochemical nature.

Ultraviolet-Visible (UV-Vis) Analysis

The UV-Vis Spectrophotometer U-2900 HITACHI was utilized to analyze silver nanoparticles, employing the principle of surface Plasmon resonance. The analysis covered a wavelength range of 250-750 nm. Notably, a wavelength of 410 nm indicated the presence of nanoparticles, with the instrument generating absorption spectra (Figure 1).

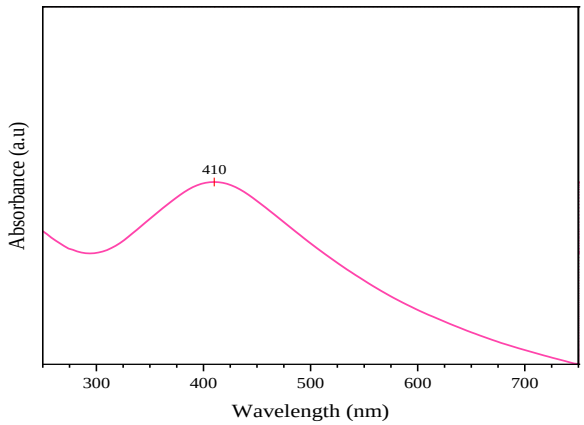

Figure 1. UV-Visible spectra of *Glycine max*-Derived Nanoparticles.

Size Distribution and Zeta Potential

The size distributions of silver nanoparticles (AgNPs) synthesized through biosynthesis were notably larger (Figure 2A). In particular, the zeta sizer of AgNPs in the aqueous extract measured 351.8 ± 146.54 nm, with a polydispersity index of 37.6%.

The zeta potential of silver nanoparticles (AgNPs) synthesized through biosynthesis was found to be

significantly high (Figure 2B). Specifically, the zeta potential of AgNPs in the aqueous extract was measured to be -7.6 ± 0.6 mV. The negative charge of AgNPs allows them to disperse in the medium, preventing aggregation. A negative charge for zeta potential specifies that the particles stay highly stable and repel each other, reducing the likelihood of clumping together.[13]

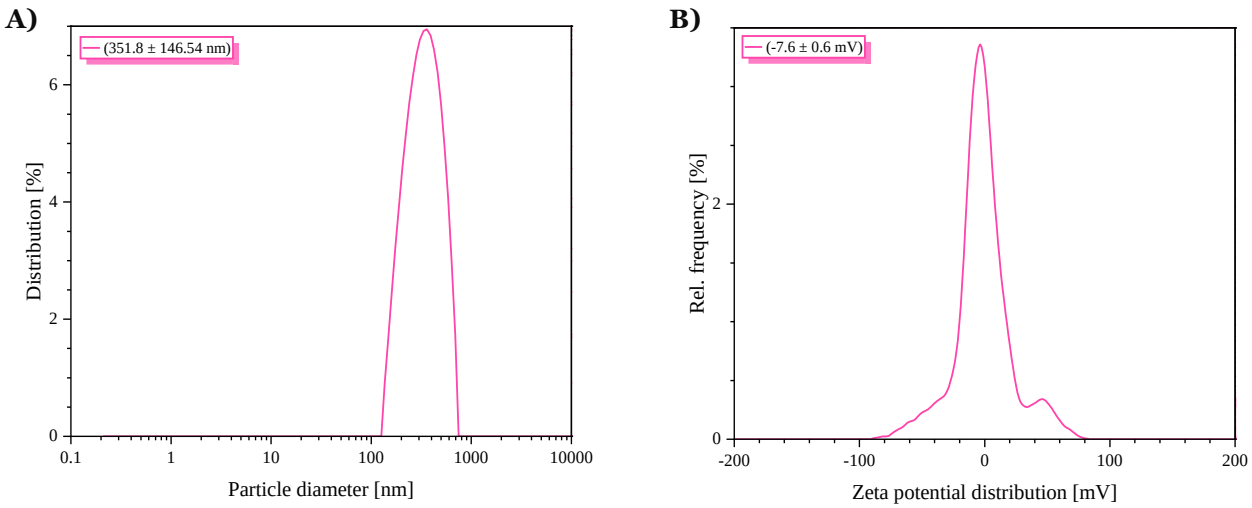

Figure 2. A) Size distributions of *Glycine max*-Derived Nanoparticles; **B)** Zeta potential of *Glycine max*-Derived Nanoparticles.

FT-IR Analysis

FT-IR Analysis was accompanied to identify the chemical compounds and functional compounds present in the nanoparticles derived from *Glycine max*. The IR spectrum of these nanoparticles, (Figure 3), were utilized for this purpose.

Glycine max-derived NPs have 4 strong FTIR spectral transmittance troughs at 0927 cm^{-1}, 1637 cm^{-1}, 2175 cm^{-1} and 3345 cm^{-1} regions, respectively.

The FTIR analysis revealed distinct peaks indicative of molecular functionalities present in the sample. The prominent peak observed at 3345 cm^{-1} indicating the presence of an aliphatic primary amine, evident from the -NH stretching vibration in the range of 3300-3500 cm^{-1}, with a dominant peak centered around 3345 cm^{-1}. Additionally, the spectrum exhibits feature associated with an aromatic secondary amine, manifested by an intense >N-H stretching vibration, typically within the same spectral region as the primary amine stretch. Moreover, the presence of normal "polymeric" -OH groups is noted, characterized by a distinct peak at 3345 cm^{-1} in the single bond region, indicative of -OH stretching vibrations commonly found in polymeric structures.

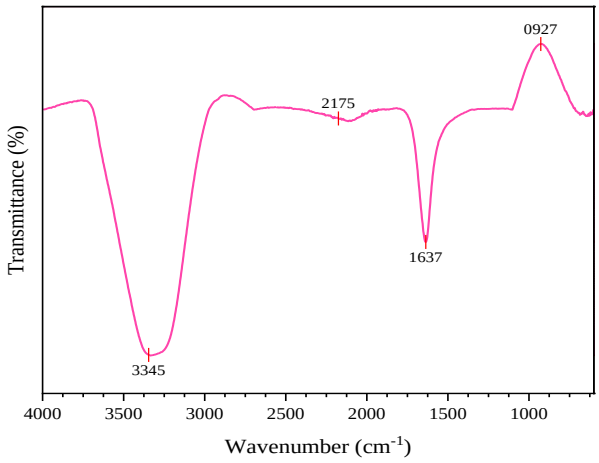

Figure 3. FT-IR Spectra of *Glycine max*-Derived Nanoparticles.

Table 1. FT-IR Absorption band of *Glycine max*-Derived Nanoparticles.

Sr.#	Absorption band of *Glycine max*-derived nanoparticles (cm^{-1})	Absorption band from Literature (cm^{-1})	Ref
01	3345	3448	14-17
02	2175	2175	
03	1637	1645	
04	0927	1034	

Another notable peak detected at 2175 cm^{-1} specifies the existence of the Thiocyanate (-SCN) functional group, representing the stretching vibration caused carbon-nitrogen triple bond (C≡N) within thiocyanate. An evident peak around 1637 cm^{-1} indicates double bonds or aromatic compounds, typical of conjugated systems, while supporting the presence of organic nitrates through associated vibrational modes, aiding in compound characterization. Additionally, the peak at 0927 cm^{-1} indicates cyclohexane ring vibrations, corresponding to bending or deformation within the ring structure, suggesting the presence of cyclohexane moieties in the sample, potentially indicating compounds or materials containing cyclohexane (Table 1).

SEM-EDX Analysis

An advanced imaging technique referred to Scanning electron microscopy in conjunction via energy dispersive X-ray spectroscopy was employed to assess both the surface characteristics and elemental conformation of the synthesized *Glycine max*-Derived Nanoparticles. The photomicrograph of *GM*-NPs exhibited a broad size distribution within the sample; the observed *GM*-NPs displayed a cubo-rhombic dodecahedral morphology (Figure 4).

In spectrum 01, the quantity of Ag was 11.84% correspondingly, whereas in spectrum 02, the percentages were 14.87%, measured in atomic % respectively. Details of the two EDX spectra of AgNPs values accessed in atomic weight % were (Table 2).

Composition, purity, besides average crystallite size of *Glycine max*-Derived Nanoparticles (Figure 5). The analysis was performed over a 2θ range of 30 to 80 degrees. The resulting pattern exhibited multiple peaks at 2θ values of 38.01°, 44.11°, 64.31°, and 77.32°. Notably, the reflection at (111), (200), (220), and (311) indicated the absence of impurities, signifying a pure anatase phase and a high crystalline nature of silver metal within the sample with the standard powder diffraction card of JCPDS Silver: 04-0783.

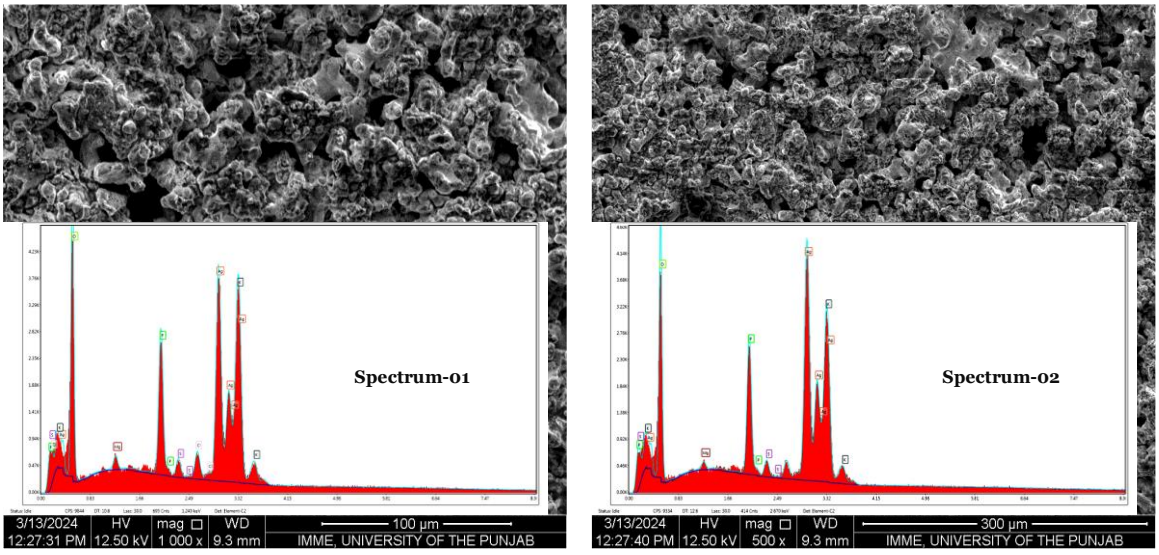

Figure 4. EDX Pattern of *Glycine max*-Derived Nanoparticles.

Table 2. EDX Weight Ration of *Glycine max*-Derived Nanoparticles.

***Glycine max*-Derived Nanoparticles**	**Element (Ag)**	
	Weight %	Atomic %
Spectrum 1	38.89	11.84
Spectrum 2	45.65	14.87

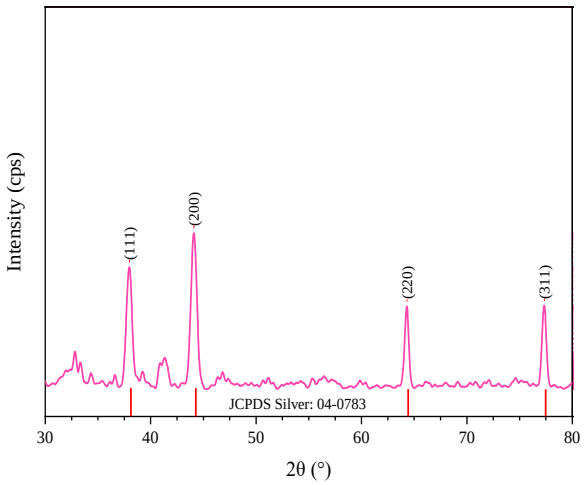

Figure 5. XRD pattern of *Glycine max*-Derived Nanoparticles.

Utilizing the Scherrer equation D = Kλ/(*βcos*(θ)), the average crystallite size of the *Glycine max*-Derived Nanoparticles was determined. The analysis revealed an average crystallite size falling within the range of 20-35 nm. However, it's worth noting that due to the synthesis method employed, there exists a slight variance between the crystallite size and the strength of the observed peaks.

Treatment of Cell Line with *Glycine max*-Derived Nanoparticles

Morphology of Hepatocellular Carcinoma Cells (HepG2)

HepG2 cell line was used for *in-vitro* analysis of Hepatocellular Carcinoma treatment with *Glycine max*-derived Nanoparticles, phase contrast microscopy was utilized for the images captured of treatments and untreated HepG2. Untreated HepG2 showed well matured, fibroblastic colonies and smooth morphology. Whereas, the treated HepG2 with *Glycine max*-derived Nanoparticles cells displayed unclear and rough morphological appearance, which confirms the anti-proliferative effect. In contrast with the control, treated group conveyed that the apoptosis was occurred in many due to the ROS production in the process, this result may occurred due to the ROS production that ultimately damaged the internal membranes (Figure 6).

MTT Assessment

Cultured HepG2 cells (500 cells per well of a 96-well plate) underwent preconditioning. Upon treatment with *Glycine max*-derived nanoparticles, cell proliferation was observed across all experimental groups. Proliferation rates were assessed using MTT reagent, revealing a significantly lower proliferation in the treated groups: *GM*-NPs 10 µg/ml (1.003 ± 0.0594), *GM*-NPs 20 µg/ml (0.529 ± 0.0092), *GM*-NPs 30 µg/ml (0.605 ± 0.0040), compared to the untreated cell group (1.291 ± 0.0029) (Figure S2).

Assessment of Dead Cells with Trypan Blue Dye

Trypan Blue staining highlights dead cells as black under a microscope. Preconditioning of cultured HepG2 cells (500 cells per 96-well plate) with *GM*-NPs 10 µg/ml and *GM*-NPs 20 µg/ml, followed by treatment with *GM*-NPs 30 µg/ml, resulted in cell death across all experimental groups. Compared to the untreated group (17.00 ± 0.5774), the treatment groups (*GM*-NPs 10 µg/ml (32.33 ± 1.453), *GM*-NPs 20 µg/ml (46.67 ± 1.202), and *GM*-NPs 30 µg/ml (61.00 ± 0.5774) exhibited significantly elevated numbers of dead cells (Figure 7).

Assessment of Live Cell Count with Crystal Violet Stain

For the assessment of live cell count, crystal violet stain was employed, which permeates live cells, and the absorbance of the resulting color was measured using a spectrophotometer. Preconditioning of cultured HepG2 cells (500 cells per well of a 96-well plate) was carried out. It was noted that there was a noticeable decrease in live cell count in the treated groups: *GM*-NPs 10 µg/ml (2.898 ± 0.0618), *GM*-NPs 20 µg/ml (2.243 ± 0.0474), *GM*-NPs 30 µg/ml (1.84 ± 0.0146), compared to the untreated cell group (3.834 ± 0.0709) (Figure S3).

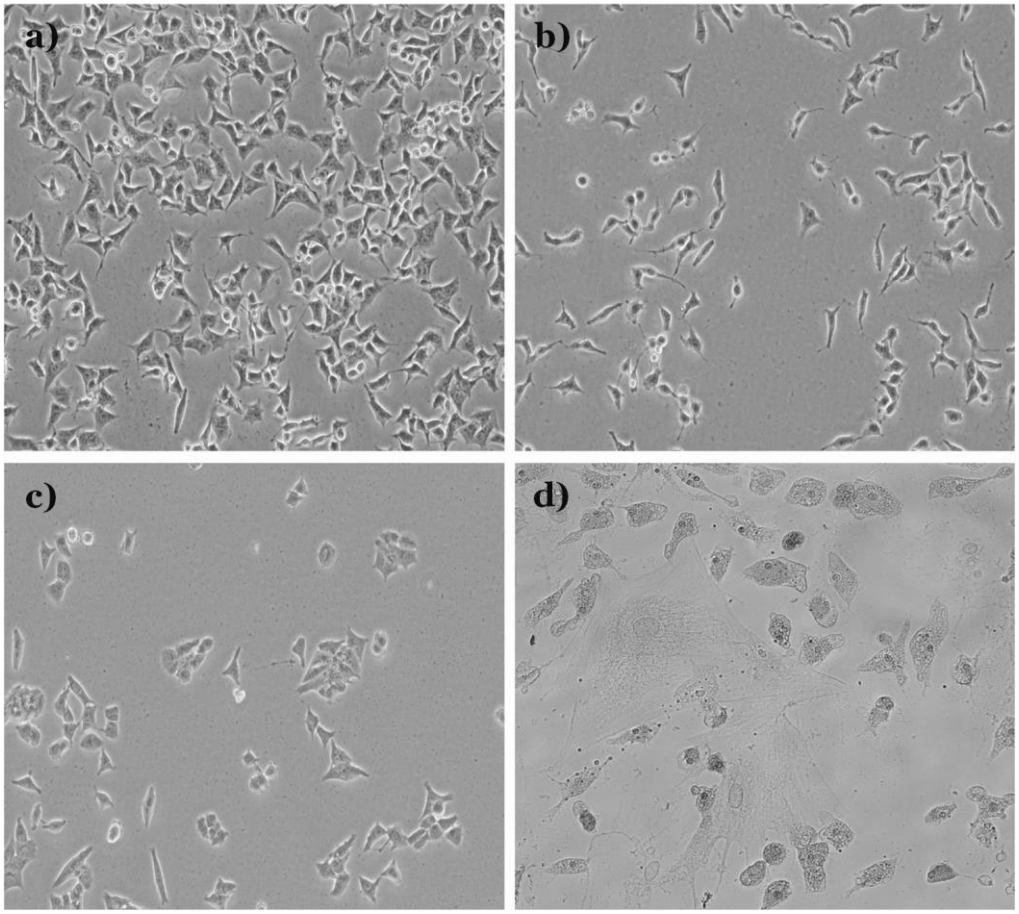

Figure 6. Morphological Appearance of HepG2 Cells. **a)** At 80% confluency, untreated HepG2 Cells shown clean, smooth morphology under a 20X phase contrast microscope; **b)** At 60% confluency, treated HepG2 Cells with *GM*-NPs 10 µg/ml after 24 hrs shown decreased viability and morphology changes under a 20X phase contrast microscope; **c)** At 40% confluency, treated HepG2 Cells with *GM*-NPs 20 µg/ml after 24 hrs shown decreased viability and morphology changes under a 20X phase contrast microscope; **d)** At 20% confluency, treated HepG2 Cells with *GM*-NPs 30 µg/ml after 24 hrs shown decreased viability and great change in morphology result in cancerous cells death under a 40X phase contrast microscope.

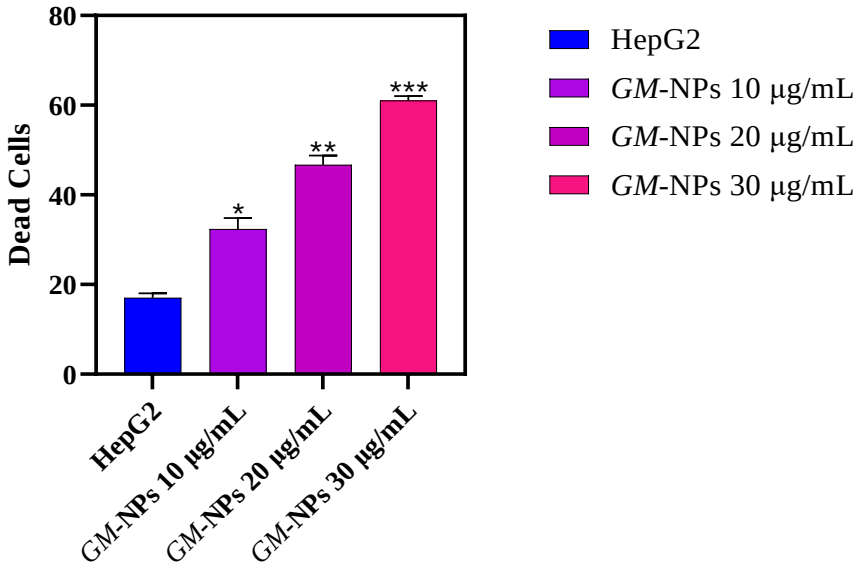

Figure 7. Cell Viability Assay: Number of dead cells (HepG2) were counted by incubating cells with trypan blue dye. Bar graph shows that HepG2 cells treated with *GM*-NPs 20 µg/ml and *GM*-NPs 30 µg/ml had significantly more dead cells than the control group. Values are mean ± SEM (P<0.05, with ** and *** indicate significant variations between control and treatment groups).

Effect on Angiogenesis of Cancer and Normal Cells

HepG2 cell line culture media were utilized for ELISA assays, employing two distinct antibodies: VEGF and Annexin V. Cells were subjected to varying concentrations of *GM*-NPs (10 µg/ml, 20 µg/ml, and 30 µg/ml). Notably, in the HepG2 cell line, the VEGF level significantly decreased with *GM*-NPs at 30 µg/ml (0.4345 ± 0.1110) (Figure 8A). Conversely, the Annexin V levels in cells treated with *GM*-NPs at 30 µg/ml exhibited marked significance (1.746 ± 0.0557), (Figure 8B). ELISA assay targeting proliferation and apoptotic markers proved that the nanoparticle could induce HCC cells, apoptotic cell death.

Interpretation of Cellular Injury through Lactate Dehydrogenase (LDH)

After exposing HepG2 cells to *GM*-NPs at concentrations of 10 µg/ml, 20 µg/ml, and 30 µg/ml, the extent of injury to the hepatocellular carcinoma cells was assessed through LDH, an enzyme that is released in response to cell injury or damage. Our findings revealed that LDH release was notably higher in cancer cells treated with *GM*-NPs at 10 µg/ml (0.9300 ± 0.0300) and *GM*-NPs 20 µg/ml (2.705 ± 0.0050) compared to untreated cells (0.4050 ± 0.0050) (Figure S4). After *GM*-NPs treatment that showed cell injury also corroborated the cytotoxic effect of the nanoparticles on cancer cells.

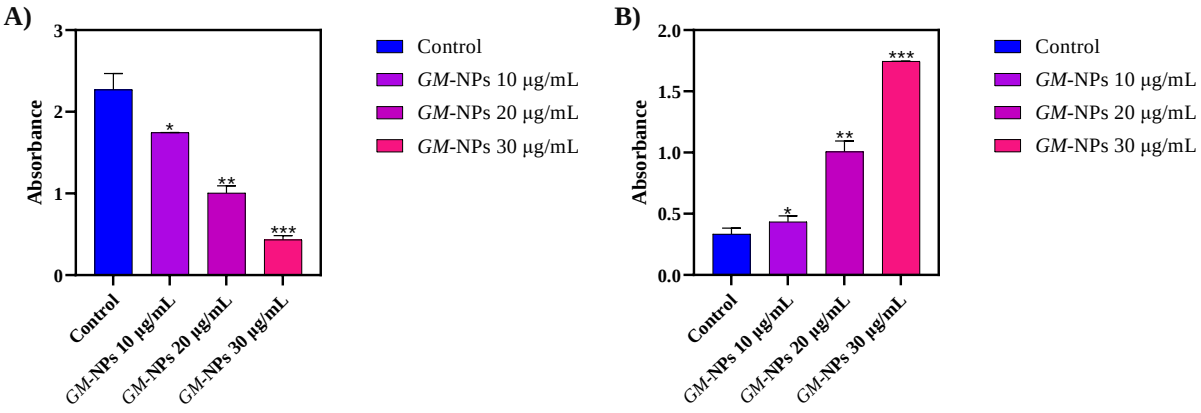

Figure 8. A) Level of VEGF in different treatment groups. Bar graph shows levels of VEGF in intra-group. Values were articulated as mean ± SEM (treated groups with *, ** and ***P<0.05). **B)** Level of Annexin-V in different treatment groups. Bar graph shows levels of Annexin V in intra-group. The values are expressed as the mean ± SEM (P<0.05, where *, ** and *** indicates a statistically significant distinction between the control and therapeutic groups).

Discussion

Hepatocellular carcinoma (HCC) is a major global health concern, with limited treatment options and a poor prognosis.[18] In recent years, bioinspired nanoparticles have materialised a promising approach for cancer therapy thanks to their distinct physicochemical attributes and potential for targeted drug delivery.[19] In current the study, an innovative green synthesis method for silver nanoparticles (AgNPs) utilizing *Glycine max* (soybean) pods as a reducing and stabilizing agent, and evaluate their anti-proliferative and apoptotic effects on HCC cells. Therefore, *Glycine max*-derived nanoparticles effectively treat liver cancer cells by promoting apoptosis and decreasing proliferation, while still being safe for non-cancerous cells.

The UV-Vis spectra at 410 nm confirmed the formation of bioinspired nanoparticles.[14] The bio-reduction of Ag^{+} ions in *Glycine max* pods extract occurs through electrostatic interactions with phytochemicals, forming silver nuclei and synthesizing AgNPs through further reduction and accumulation.[20] The zeta size of the extract measured 351.8 ± 146.54 nm, with a polydispersity index of 37.6%.[21]

While the Zeta potential measured -7.6 mV ± 0.6 mV.[13] The 4 strong IR spectral transmittance troughs at 0927 cm^{-1}, 1637 cm^{-1}, 2175 cm^{-1} and 3345 cm^{-1} regions, respectively.[14-17] SEM-EDX analysis reveals surface morphology and elemental composition, with spectrum 01 containing 11.84% Ag and spectrum 02 having 14.87% Ag in atomic percentage.[22] XRD analysis revealed a pure anatase phase and high crystalline nature of silver metal in *Glycine max*-derived nanoparticles, indicating no impurities at the reflection at (111), (200), (220), and (311) indicated the absence of impurities.[23-25]

In-vitro analysis of Hepatocellular Carcinoma

treatment with *Glycine max*-derived nanoparticles revealed anti-proliferative effect, with apoptosis observed in many treated cells due to ROS production.[26,27] Cell proliferation was observed in HepG2 cells treated with *Glycine max*-derived nanoparticles, with significantly lower rates in the treated groups associated to the untreated group.[28,29] Cell death was observed in HepG2 cells preconditioned with *GM*-NPs, with treatment groups showing significantly higher numbers of dead cells compared to untreated groups.[30,31]

Crystal violet stain was used to assess live cell count in preconditioning HepG2 cells. Treatment groups showed a significant decrease in live cell count compared to untreated cells.[32,33] The VEGF level significantly decreased with *GM*-NPs at a concentration of 30 µg/ml in the HepG2 cell line. The study found that cells treated with *GM*-NPs at a concentration of 30 µg/ml showed ominously higher Annexin V levels.[34,35] The nanoparticle was found to induce apoptosis in HCC cells through an ELISA assay targeting proliferation and apoptotic markers.[36]

The study found that *GM*-NPs treatment significantly increased LDH release in HepG2 cancer cells, indicating a potential therapeutic approach for hepatocellular carcinoma.[37,38] The treatment of *GM*-NPs with cancer cells demonstrated cell injury, confirming the cytotoxic effect of these nanoparticles on cancer cells.[39]

Glycine max-derived nanoparticles pave a cost-effective and innovative approach for hepatocellular carcinoma, aligning with SDGs 3 for good health and well-being. *Glycine max*-derived nanoparticles may work synergistically to trigger apoptosis within liver cancer cells. The potential regarding *Glycine max*-derived nanoparticles to induce apoptosis is enhanced by their ability to modify gene expression and sensitize cancer cells to apoptosis. Furthermore, the anti-inflammatory and antioxidant properties of *Glycine max*-derived nanoparticles may maximize therapeutic benefits while reducing side effects.

Conclusion

In conclusion, this study successfully synthesized and characterized green-synthesized nanoparticles. The nanoparticles in *Glycine max* that were synthesized and confirmed by UV-vis spectrophotometry and associated groups of particles, morphologies, and composition structures were analysed by FTIR and SEM-EDX. Furthermore, XRD examination determined the phase composition, purity, and average crystallite of specimens and particle size distribution and Zeta potential examination were also performed. The anticancer ability of the green synthesized NPs against the HepG2 cancer cell line was reported to be promising and was proven to be treated with nanoparticles synthesized from *Glycine max*.

Conflict of Interest

The authors declare no conflicts of interest.

Ethical Approval

According to Centre of Excellence in Molecular Biology (CEMB) is a highly distinguished biological research institute in Asia, located on the West Bank of the picturesque Canal Road Lahore, Punjab, Pakistan. It is an autonomous organization that is under administrative control of University of the Punjab, Lahore, Pakistan. This study was carried out using commercially available human cancer cell lines, which are exempt from further ethical approval requirements. The HepG2 cell line was purchased by the university from the biorepository American Type Culture Collection (ATCC) provided the authentic cell lines used in this investigation, which were managed in compliance with Good Laboratory Practice (GLP) guidelines.

Acknowledgement

We would like to extend our sincere appreciation to the Department of Chemistry at the University of Engineering and Technology, Lahore, for their invaluable support and resources throughout this research project. We extend our appreciation to all individuals who provided assistance and guidance, contributing significantly to the successful completion of this work. Special thanks are due to our parents for their unwavering support and encouragement, which have been instrumental in our academic and research endeavors. Their hard work and dedication have been a constant source of inspiration.

References

1. Priya K, Vijayakumar M, Janani B. Chitosan-mediated synthesis of biogenic silver nanoparticles (AgNPs), nanoparticle characterisation and in vitro assessment of anticancer activity in human hepatocellular carcinoma HepG2 cells. Int J Biol Macromol. 2020;149:844-52. doi:10.1016/j.ijbiomac.2020.02.007
2. Baig N, Kammakakam I, Falath W. Nanomaterials: A review of

synthesis methods, properties, recent progress, and challenges. Mater Adv. 2021;2(6):1821-71. doi:10.1016/j.ijbiomac.2020.02.007
3. Patra JK, Gouda S. Application of nanotechnology in textile engineering: An overview. J Eng Technol Res. 2013;5(5):104-11.
4. Sharma A, Yadav MK, Vidhya CS, Kumar KA, Khatana K, Panik RK, et al. Nanomaterials and nanotechnology: a comprehensive study of synthesis, characterization and multifaceted applications. Biochem Cell Arch. 2023;23.
5. Kitisin K, Packiam V, Steel J, Humar A, Gamblin TC, Geller DA, et al. Presentation and outcomes of hepatocellular carcinoma patients at a western centre. HPB. 2011;13(10):712-22. doi:10.1111/j.1477-2574.2011.00362.x
6. Lee SH, Song IH, Noh R, Kang HY, Kim SB, Ko SY, et al. Clinical outcomes of patients with advanced hepatocellular carcinoma treated with sorafenib: a retrospective study of routine clinical practice in multi-institutions. BMC Cancer. 2015;15:236. doi:10.1186/s12885-015-1273-2
7. Huang Y, Mei C, Tian Y, Nie T, Liu Z, Chen T. Bioinspired tumor-homing nanosystem for precise cancer therapy via reprogramming of tumor-associated macrophages. NPG Asia Mater. 2018;10(10):1002-15. doi:10.1038/s41427-018-0091-9
8. Shea Z, Ogando do Granja M, Fletcher EB, Zheng Y, Bewick P, Wang Z, et al. A Review of Bioactive Compound Effects from Primary Legume Protein Sources in Human and Animal Health. Curr Issues Mol Biol. 2024;46(5):4203-33. doi:10.3390/cimb46050257
9. Huang C, Quan X, Yin Y, Ding X, Yang Z, Zhu J, et al. Enrichment of Flavonoids in Short-Germinated Black Soybeans (*Glycine max* L.) Induced by Slight Acid Treatment. Foods. 2024;13(6):868. doi:10.3390/foods13060868
10. Hublikar LV, Ganachari SV, Patil VB, Nandi S, Honnad A. Anticancer potential of biologically synthesized silver nanoparticles using *Lantana camara* leaf extract. Prog Biomater. 2023;12(2):155-69. doi:10.1007/s40204-023-00219-9
11. Shaaban MT, Mohamed BS, Zayed M, El-Sabbagh SM. Antibacterial, antibiofilm, and anticancer activity of silver-nanoparticles synthesized from the cell-filtrate of *Streptomyces enissocaesilis*. BMC Biotechnol. 2024;24(1):8. doi:10.1186/s12896-024-00833-w
12. Liu X, Chen JL, Yang WY, Qian YC, Pan JY, Zhu CN, et al. Biosynthesis of silver nanoparticles with antimicrobial and anticancer properties using two novel yeasts. Sci Rep. 2021;11(1):15795. doi:10.1038/s41598-021-95262-6
13. Ejaz U, Afzal M, Mazhar M, Riaz M, Ahmed N, Rizg WY, et al. Characterization, synthesis, and biological activities of silver nanoparticles produced via green synthesis method using *Thymus vulgaris* aqueous extract. Int J Nanomed. 2024:453-69.
14. Prasad C, Venkateswarlu P. Soybean seeds extract based green synthesis of silver nanoparticles. Indian J Adv Chem Sci. 2014;2(3):208-11. doi:10.1007/s12257-012-0021-6
15. Sasikala D, Govindaraju K, Tamilselvan S, Singaravelu G. Soybean protein: a natural source for the production of green silver nanoparticles. Biotechnol Bioprocess Eng. 2012;17:1176-81.
16. Nandiyanto AB, Oktiani R, Ragadhita R. How to read and interpret FTIR spectroscope of organic material. Indones J Sci Technol. 2019;4(1):97-118.
17. Md IU, Kalyani D, Tejasri N, Mounika A, Sowndarya A, Anitha J, et al. Green Synthesis and Characterization of Silver Nanoparticles using Glycine Max L. Seed Extract and their Antiepileptic Activity in Rats. Int J Pharm Sci Nanotechnol. 2017;10(6):3909-14. doi:10.37285/ijpsn.2017.10.6.6
18. Pina-Sanchez P, Chavez-Gonzalez A, Ruiz-Tachiquin M, Vadillo E, Monroy-Garcia A, Montesinos JJ, et al. Cancer biology, epidemiology, and treatment in the 21st century: current status and future challenges from a biomedical perspective. Cancer Control. 2021;28:10732748211038735. doi:10.1177/10732748211038735
19. Hongbao M, Ma M, Yan Y. Cancer Biology Research Literatures. Cancer Biol. 2015;5(2):79-95. doi:10.7537/marscbj070215.08
20. Riaz M, Ismail M, Ahmad B, Zahid N, Jabbour G, Khan MS, et al. Characterizations and analysis of the antioxidant, antimicrobial, and dye reduction ability of green synthesized silver nanoparticles. Green Process Synth. 2020;9(1):693-705. doi:10.1515/gps-2020-0064
21. Oliveira LS, Furtado LL, Diniz FD, Mendes BL, Araújo TR, Silva LP, et al. Eco-Friendly Silver Nanoparticles Synthesized from a Soybean By-Product with Nematicidal Efficacy against *Pratylenchus brachyurus*. Nanomaterials. 2023;14(1):101. doi:10.3390/nano14010101
22. Hairil Anuar AH, Abd Ghafar SA, Hanafiah RM, Lim V, Mohd Pazli NF. Critical Evaluation of Green Synthesized Silver Nanoparticles-Kaempferol for Antibacterial Activity Against Methicillin-Resistant *Staphylococcus aureus*. Int J Nanomedicine. 2024:1339-50.
23. Hernandez-Viezcas JA, Castillo-Michel H, Andrews JC, Cotte M, Rico C, Peralta-Videa JR, et al. In situ synchrotron X-ray fluorescence mapping and speciation of CeO2 and ZnO nanoparticles in soil cultivated soybean (Glycine max). ACS Nano. 2013;7(2):1415-23. doi:10.1021/nn305196q
24. Petla RK, Vivekanandhan S, Misra M, Mohanty AK, Satyanarayana N. Soybean (*Glycine max*) leaf extract based green synthesis of palladium nanoparticles. J Biomater Nanobiotechnol. 2012;3(1):16695. doi:10.4236/jbnb.2012.31003
25. Ali MH, Azad MA, Khan KA, Rahman MO, Chakma U, Kumer A. Analysis of crystallographic structures and properties of silver nanoparticles synthesized using PKL extract and nanoscale characterization techniques. ACS Omega. 2023;8(31):28133-42. doi:10.1021/acsomega.3c01261
26. Buskaran K, Hussein MZ, Mohd Moklas MA, Fakurazi S. Morphological changes and cellular uptake of functionalized graphene oxide loaded with protocatechuic acid and folic acid in hepatocellular carcinoma cancer cell. Int J Mol Sci. 2020;21(16):5874. doi:10.3390/ijms21165874
27. Monga J, Pandit S, Chauhan RS, Chauhan CS, Chauhan SS, Sharma M. Growth inhibition and apoptosis induction by (+)-Cyanidan-3-ol in hepatocellular carcinoma. PLoS One. 2013;8(7):e68710. doi:10.1371/journal.pone.0068710
28. Twarużek M, Zastempowska E, Soszczyńska E, Ałtyn I. The use of in vitro assays for the assessment of cytotoxicity on the example of MTT test; 2019.
29. Manoochehri Z, Etebari M, Pannetier P, Ebrahimpour K. In vitro toxicity of polyethylene terephthalate nanoplastics (PET-NPs) in human hepatocarcinoma (HepG2) cell line. J Toxicol Environ Health Sci. 2024:203-15. doi:10.1007/s13530-024-00213-z
30. El-Dabae WH. Efficiency of MTT and Trypan Blue Assays for Detection of Viability and Recovery of Different Frozen Cell Lines. Egypt J Vet Sci. 2024;55(6):1649-57. doi:10.21608/ejvs.2024.260687.1764
31. Althafar ZM. Evaluation of Anti-proliferative and Antioxidant Potency of *Ficus benghalensis* Hydroalcoholic Bark Extract against Lung Cancer Cell Line-A549. Ind J Pharm Edu Res. 2024;58(2):510-8.
32. Talebipour A, Saviz M, Vafaiee M, Faraji-Dana R. Facilitating long-term cell examinations and time-lapse recordings in cell biology research with CO2 mini-incubators. Sci Rep. 2024;14(1):3418. doi:10.1038/s41598-024-52866-y
33. Khalef L, Lydia R, Filicia K, Moussa B. Cell viability and cytotoxicity assays: Biochemical elements and cellular compartments. Cell Biochem Funct. 2024;42(3):e4007. doi:10.1002/cbf.4007
34. Sun X, Gao W, Liu Y, Wang Y, Wei C, Shan L, et al. pH-responsive morphology shifting peptides coloaded with paclitaxel and sorafenib inhibit angiogenesis and tumor growth. Mater Des. 2024;238:112619. doi:10.1016/j.matdes.2023.112619
35. Sulukoğlu EK, Günaydın Ş, Kalın ŞN, Altay A, Budak H. Diffractaic acid exerts anti-cancer effects on hepatocellular carcinoma HepG2 cells by inducing apoptosis and suppressing migration through targeting thioredoxin reductase 1. Naunyn Schmiedebergs Arch Pharmacol. 2024;379:5745-55.. doi:10.1007/s00210-024-02980-5
36. Grijalva M, Vallejo-López MJ, Salazar L, Camacho J, Kumar B. Cytotoxic and antiproliferative effects of nanomaterials on cancer cell lines: a review. Unraveling the Safety Profile of Nanoscale Particles and Materials—From Biomedical to Environmental Applications. 2018:63-85.
37. Mickymaray S. Molecular Mechanism of Apoptotic Cell Death in Cyanidin-3-glucoside-induced Cytotoxic Potential on Human Liver Carcinoma (HepG2) Cell Line. Ind J Pharm Edu

Res. 2024;58(1):254-62. doi:10.5530/ijper.58.1.27
38. Carrão Dantas EK, Ferreira CL, da Cunha Goldstein A, da Silva Fernandes A, Anastacio Ferraz ER, Felzenszwalb I, et al. Marketable 1, 3-dimethylamylamine and caffeine-based thermogenic supplements: Regulatory genotoxicity assessment through in vitro and in silico approaches. J Toxicol Environ Health Part A. 2024;87(6):245-65. doi:10.1080/15287394.2023.2294925
39. Volovat SR, Negru S, Stolniceanu CR, Volovat C, Lungulescu C, Scripcariu D, et al. Nanomedicine to modulate immunotherapy in cutaneous melanoma. Exp Ther Med. 2021;21(5):535. doi:10.3892/etm.2021.9967